Available online at www.sciencedirect.com
ScienceDirect
Carbohydrate Research 342 (2007) 2192–2201
Carbohydrate RESEARCH

Binding of glycosaminoglycans to cyano-activated agarose membranes: kinetic and diffusional effects on yield and homogeneity

Kristin J. Mattern and William M. Deen*

Department of Chemical Engineering, Massachusetts Institute of Technology, 77 Massachusetts Avenue, Cambridge, MA 02139, USA

Received 26 January 2007; received in revised form 29 May 2007; accepted 4 June 2007
Available online 12 June 2007

Abstract—Methods were developed for binding a glycosaminoglycan (GAG, a 50 kDa chondroitin sulfate) to thin agarose membranes using 1-cyano-4-(dimethylamino)pyridinium tetrafluoroborate (CDAP) as the activating agent. Process conditions were optimized to achieve high yields and spatially uniform concentrations of bound ligand. Yields were varied mainly by manipulating the duration and temperature of the aqueous washes prior to coupling, which affected the concentration of active sites available for subsequent GAG binding. The rate constants for degradation of the active cyanate esters in 0.1 M bicarbonate solutions were $0.24 \pm 0.02\ h^{-1}$ at 4 °C and $0.08 \pm 0.03\ h^{-1}$ at 0 °C. Steric limitations in the 3% agarose gels severely restricted binding, with only about 0.1% of active sites being accessible to GAG molecules. The GAG binding occurred primarily in the outer 50–70 μm of the membranes, so that coupling was homogeneous only for thin gels. A model of GAG diffusion and reaction in the coupling step was developed to explain the observed effects of parameters such as the GAG concentration in solution and the membrane thickness. An analysis of the key time scales in the synthesis provides design principles that should be useful also for other cyanylating agents, other ligands, and for beads as well as membranes.

Keywords: 1-Cyano-4-(dimethylamino)pyridinium tetrafluoroborate (CDAP); Agarose activation; Glycosaminoglycans; Chondroitin sulfate; Cyanate ester degradation kinetics; Reaction–diffusion model

1. Introduction

Numerous technologies make use of ligands bound to carbohydrate substrates, and many attachment techniques are available.[1–3] One common approach couples an amino group on the ligand [protein, polynucleotide, peptide, glycosaminoglycan (GAG), etc.] to an activated site on the carbohydrate.[4] This strategy has been used for the preparation of affinity chromatography beads, DNA and protein micro arrays, and conjugate vaccines, to cite a few examples.[5–8]

One common coupling method uses agarose that has been activated by cyanogen bromide (CNBr) or similar agents to turn hydroxyl groups into cyanate esters, which react readily with the primary amines found on ligands.[4,9–11] Since the discovery of the cyanogen halide method for coupling proteins to polysaccharides in 1967,[9,12] a number of improvements in the activation method have been made, as reviewed by Kohn and Wilchek.[4] While CNBr is still often used, several other cyanylating agents discovered in the early 1980s pose a less severe health risk and increase the activation yield. Three of note are *N*-cyanotriethylammonium tetrafluoroborate (CTEA), *p*-nitrophenylcyanate (pNPC), and 1-cyano-4-(dimethylamino)pyridinium tetrafluoroborate (CDAP). While the three reagents are similar in structure and reaction sequence, CDAP has the advantage of not requiring temperatures below 0 °C and giving activation yields at least three to eight times higher than CTEA, pNPC, or CNBr.[4]

* Corresponding author. Fax: +1 617 253 2072; e-mail: wmdeen@mit.edu

0008-6215/$ - see front matter © 2007 Elsevier Ltd. All rights reserved.
doi:10.1016/j.carres.2007.06.007

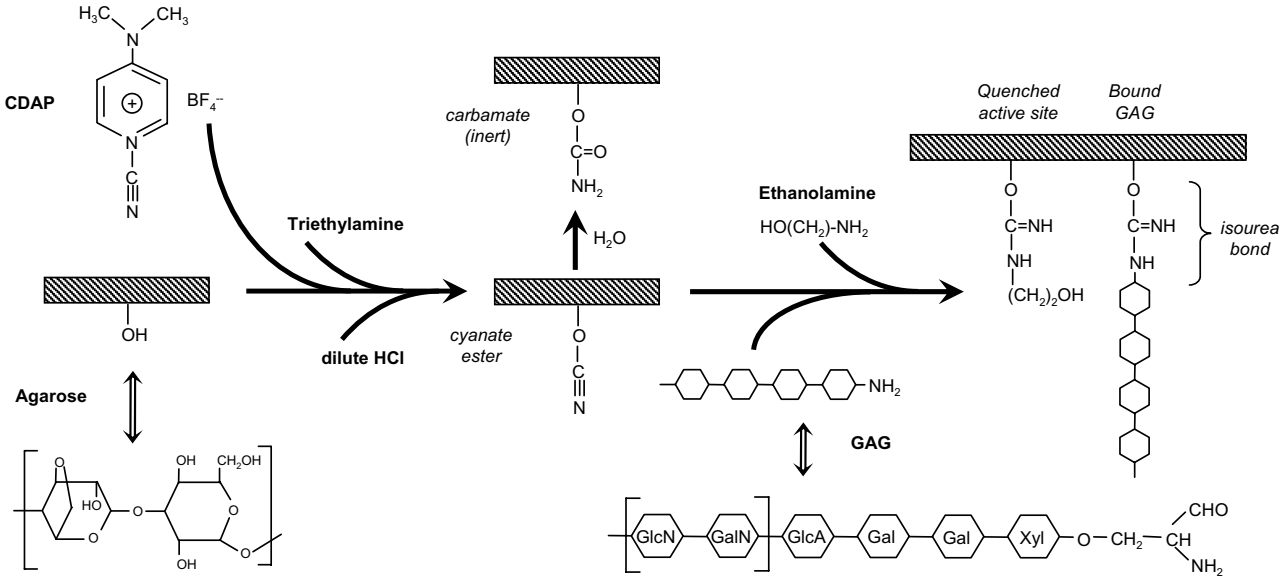

Figure 1. Reaction pathway for the activation of agarose by CDAP and the binding of GAG, based on the mechanism proposed by Kohn and Wilcheck.[4]

The CDAP reaction sequence is shown in Figure 1. When CDAP and triethylamine (a cyano-transfer agent) are added, the agarose hydroxyl groups are converted to a pyridinium–isourea derivative. In slightly acidic conditions, the equilibrium of the isourea derivative is shifted toward the cyanate ester. In the presence of primary amines (such as the terminal peptide of a GAG or a small quench molecule like ethanolamine), the amine and cyanate ester form an isourea bond. There are several competing reactions. In aqueous conditions, the cyanate ester can degrade into an inert carbamate group. It can also form imidocarbonate bonds with other activated groups, forming a cyclic bond between neighboring active groups or a linear bond that cross-links two agarose fibers.

The objective of the present work was to adapt previously reported activation and coupling procedures to prepare agarose–GAG membranes with end-on binding of the GAG chains to the agarose fibrils. Such membranes will be used by us in the future to measure the hydraulic permeability and protein sieving characteristics of GAG matrices, as they relate to microvascular permeability. To achieve the desired permeability properties, the membranes needed a high GAG concentration and a homogeneous distribution of GAG throughout the membrane volume. Maximizing coupling yields while maintaining homogeneity required an understanding of what factor(s) limit GAG binding in the coupling procedures. While others have mentioned reaction conditions that may improve or detract from ligand attachment to cyano-activated Sepharose® beads or dextran, no systematic study has been reported. Potential limiting parameters for ligand coupling were studied both experimentally and through modeling to determine reaction conditions that create a membrane with a high, homogeneous concentration of bound GAG. The mechanistic insight so obtained provides insight into how to optimize syntheses involving other ligands, other cyanylating agents, and other resin geometries (such as beads).

2. Experimental

2.1. Materials

All chemicals were of reagent grade or higher. A high-molecular-weight chondroitin sulfate was used as the GAG, unless otherwise specified. The attachment chemistry required the GAG to contain a protein residue with a primary amine. Chondroitin sulfate A (#230687 from bovine trachea, MW $\sim$ 50 kDa) and heparin (#375095 from porcine intestinal mucosa, MW $\sim$ 15 kDa) from Calbiochem (La Jolla, CA) were verified to contain primary amines, using a fluorescamine assay.[13–15] CDAP was purchased from Research Organics (#1458C; Cleveland, OH) and agarose from Sigma (type VI; St. Louis, MO).

2.2. Agarose membrane preparation

A 3.075 w/w % (3 v/v %) agarose solution in 0.1 M KCl–phosphate buffer (pH 7.4) was heated and used to cast agarose membranes on woven polyester supports, as described previously by our group.[16,17] The membrane diameter was 25 mm and the usual thickness was 70 μm, but for some experiments the thickness

was varied by placing glass coverslips next to the mesh as spacers or by using a thinner nylon support mesh.

2.3. Agarose activation

The agarose activation procedure with CDAP was based on the method used by Kohn and Wilchek for polysaccharide resin beads,[4] modified to allow a batch of 20 agarose membranes to be processed at one time. Two slightly different procedures were used. Procedure I produced a lower yield of bound GAG, and Procedure II a higher yield. Unless otherwise noted in the results, Procedure I was used.

Procedure I: Each agarose membrane was placed in a plastic histology cassette (Histo-prep Tissue Capsules #15-182-219; Fisher, Hampton, NH). Twenty membranes were soaked for 15 min with gentle agitation in each of the following: 1 L of deionized water, 1 L of 30% acetone (two times), and 1 L of 60% acetone (two times). In a beaker in an ice bath, the washed gels were added to 200 mL of ice-cold 60% acetone. With orbital mixing at 150–200 rpm, 20 mL of 100 mg/mL of CDAP in dry acetonitrile was added. After 1 min, 16 mL of 0.2 M Et_3N solution was added dropwise over 1–2 min. The system was mixed for an additional 5 min. The membranes were rapidly transferred to 1500 mL of refrigerated (4 °C) 0.05 N HCl (500 mL in each of three jars) and mixed for 30 min. The membranes were then soaked in 2 L of refrigerated deionized water for 15 min (three times), then immediately used for coupling.

Procedure II: The method just described was followed through the placement of the membranes in 0.05 N HCl, except that each jar of HCl contained approximately 100 mL of ice. The membranes were mixed in the HCl solution for 10 min, then soaked in 2 L of ice-water for 5 min with mixing (three times) before immediate coupling.

2.4. GAG coupling

The procedure here was based on the method used by Iverius.[10] The activated agarose membranes (in their cassettes) were covered with 1 g/L of GAG in 0.1 M $NaHCO_3$. To synthesize 'blank' membranes, the activated membranes were placed in 0.1 M $NaHCO_3$ with no GAG. The system was stirred with orbital mixing at 4 °C for at least 16 h. To remove the remaining active groups, 7.5 mL of ethanolamine was added per 100 mL of attachment solution and stirred for 4 h at 4 °C. The membranes were soaked for 15 min with gentle agitation in each of the following: 2 L of deionized water (three times), 2 L of 0.5 M NaCl (two times), and 2 L of deionized water (six times). Each gel was removed from its cassette, stored in 0.1 M KCl–phosphate buffer, and refrigerated until use.

2.5. Bound GAG assay

The assay for bound GAG was adapted from that used by Smith et al.[18] to assay heparin immobilized on Sepharose® beads, using *o*-toluidine blue dye. For a single gel, a dye solution volume of 2.5 mL and a total volume of 5 mL were used. To allow adequate time for the dye to bind, each test tube was allowed to equilibrate for at least 15 min before centrifuging. The absorbance at 631 nm was measured directly from a sample of the aqueous layer without dilution by ethanol.

The absorbance of the samples was correlated to the absorbance of the reference solutions and corrected for the blank gel absorbance to determine the bound GAG concentration. The linear calibration curves were of the form

$$M = \varepsilon A \tag{1}$$

where M is the mass of GAG in the test tube and A is the absorbance. Knowing the calibration slope (ε) and the absorbance of a blank gel (A_0), the mass of GAG in a sample (M_s) was calculated as

$$M_s = \varepsilon\left(\frac{V_s}{V_t}\right)A_s - \varepsilon\left(\frac{V_0}{V_t}\right)A_0 \tag{2}$$

where V_0 and V_s are the volumes of the blank and sample membranes, V_t is the total volume of the dye solution plus membrane, and A_s is the absorbance of the sample.

2.6. Membrane sectioning and GAG visualization

Cryosectioning of gels was used to check binding homogeneity. To minimize distortion of the agarose membranes, the gels were frozen and sectioned in 0.1 M phosphate-buffered saline (pH 7.4). The bound GAG was visualized with a 0.5 g/L *o*-toluidine blue solution in 0.1 N HCl. Several drops of the dye solution were placed on the membrane section for 15 min, then rapidly rinsed away and blotted dry. While toluidine staining is not well suited for quantitative histology, due to its nonlinearity at very low GAG concentrations, it is sufficient for indicating large variations in the bound GAG concentration of a gel.

2.7. Active-site assay

The assay for active cyanate esters is based on the *N*,*N*′-dimethylbarbituric acid method used by Kohn and Wilchek.[19] Each agarose gel was assayed with 3 mL of dimethylbarbituric acid solution.

2.8. Mathematical model of coupling

A mathematical model was developed to explain the observed effects of the coupling conditions on binding

yield and binding homogeneity, similar to the approach of Bernstein et al.[20] but without the assumption of constant active-site concentrations. The model describes the time-dependent diffusion of free GAG into a gel membrane of thickness δ, the reaction of GAG with activated sites to yield bound GAG, and the competing reaction in which the activated sites are degraded. The concentration of species i in the gel is denoted as $C_i(x,t)$, where x is the position (0 at the gel center and $\pm\delta/2$ at the surfaces), t is time, and $i = \mathrm{G}$, A, and B for free GAG, accessible active sites, and bound GAG, respectively. From local conservation of mass for each species, the concentrations are governed by

$$\frac{\partial C_\mathrm{G}}{\partial t} = \frac{\partial}{\partial x}\left(D\frac{\partial C_\mathrm{G}}{\partial x}\right) - k_1 C_\mathrm{A} C_\mathrm{G} \tag{3}$$

$$\frac{\partial C_\mathrm{A}}{\partial t} = -k_1 C_\mathrm{A} C_\mathrm{G} - k_2 C_\mathrm{A} \tag{4}$$

$$\frac{\partial C_\mathrm{B}}{\partial t} = k_1 C_\mathrm{A} C_\mathrm{G} \tag{5}$$

where D is the diffusivity of free GAG in the gel, k_1 is the rate constant for binding, and k_2 is the rate constant for active-site degradation. Eq. 3 allows D to be a function of C_B (and therefore a function of x and t), which was found to be much more consistent with the results than a constant diffusivity. The diffusivity in the absence of bound GAG (a constant) is denoted as D_0.

For ease of numerical solution, and also to better assess the competing rate processes, Eqs. 3–5 were converted to scaled dimensionless variables. Using $\delta/2$ as the length scale and $\delta^2/4D_0$ as the characteristic time, the dimensionless position (X) and time (τ) were defined as

$$X = \frac{2x}{\delta}, \quad \tau = \frac{4tD_0}{\delta^2} \tag{6}$$

The dimensionless concentration variables used were

$$\theta_\mathrm{G} = \frac{C_\mathrm{G}}{KC_\mathrm{GS}}, \quad \theta_\mathrm{A} = \frac{C_\mathrm{A}}{\phi C_\mathrm{A0}}, \quad \theta_\mathrm{B} = \frac{C_\mathrm{B}}{\phi C_\mathrm{A0}} \tag{7}$$

where C_GS is the GAG concentration in the external solution, C_A0 is the initial concentration of active sites (i.e., immediately before addition of GAG), ϕ is the fraction of the active sites that are accessible to the GAG, and K is the partition coefficient for the GAG (gel-to-solution concentration ratio at equilibrium). As shown, the GAG and active-site concentrations are each expressed relative to their maximum values, and the bound GAG concentration is relative to what it would be if all accessible active sites were utilized.

There is no precise way to predict the extent to which the bound GAG will 'clog' the gel, thereby reducing the diffusivity of the free GAG. However, based on theories for diffusion through random fiber matrices,[21] a reasonable functional form for the relative diffusivity is

$$f = \frac{D}{D_0} = \exp(-m\theta_\mathrm{B}) \tag{8}$$

where $m \geqslant 0$. In the absence of a predictive model for macromolecule diffusion through a mixture of uncharged and charged fibers of differing radii, we viewed m as an empirical parameter and chose a value that best represented our results.

Using the definitions in Eqs. 6–8, the conservation equations become

$$\frac{\partial\theta_\mathrm{G}}{\partial\tau} = \exp(-m\theta_\mathrm{B})\left(\frac{\partial^2\theta_\mathrm{G}}{\partial X^2} - m\frac{\partial\theta_\mathrm{B}}{\partial X}\frac{\partial\theta_\mathrm{G}}{\partial X}\right) - \alpha\theta_\mathrm{A}\theta_\mathrm{G} \tag{9}$$

$$\frac{\partial\theta_\mathrm{A}}{\partial\tau} = -\alpha\gamma\theta_\mathrm{A}\theta_\mathrm{G} - \beta\theta_\mathrm{A} \tag{10}$$

$$\frac{\partial\theta_\mathrm{B}}{\partial\tau} = \alpha\gamma\theta_\mathrm{A}\theta_\mathrm{G} \tag{11}$$

where α, β, and γ are constants that will be defined shortly. The initial and boundary conditions to be satisfied by $\theta_i(X,\tau)$ were

$$\theta_\mathrm{A}(X,0) = 1, \quad \theta_\mathrm{B}(X,0) = 0 = \theta_\mathrm{G}(X,0) \tag{12}$$

$$\frac{\partial\theta_\mathrm{G}}{\partial X}(0,\tau) = 0, \quad \theta_\mathrm{G}(1,\tau) = 1. \tag{13}$$

Because $X = 0$ is a symmetry plane, the boundary value problem defined by Eqs. 9–13 had to be solved only for $0 \leqslant X \leqslant 1$. The solution was obtained numerically by finite differences, using a stiff ODE solver ('*ode23s*') in MATLAB®.

The three dimensionless parameters in the boundary value problem are

$$\alpha = \frac{k_1\phi C_\mathrm{A0}\delta^2}{4D_0}, \quad \beta = \frac{k_2\delta^2}{4D_0}, \quad \gamma = \frac{KC_\mathrm{GS}}{\phi C_\mathrm{A0}} \tag{14}$$

where α is a Damköhler number that measures the rate of binding relative to GAG diffusion, β is a Damköhler number that measures the rate of active-site degradation relative to GAG diffusion, and γ is the maximum concentration of free GAG in the gel (that next to the surface) divided by the maximum concentration of accessible active sites (the initial value).

3. Results

3.1. Effect of activation conditions on yield

Using activation Procedure I, the average bound GAG concentration of the membranes was 68 ± 8 μg GAG per mg agarose (standard deviation from $n = 9$ activation batches). The only activation process parameters observed to significantly increase the bound GAG concentration of the membranes (>25% change) were the temperature and duration of the aqueous wash preceding GAG attachment. The use of well-mixed ice-water (0 °C) instead of refrigerated water (4 °C) increased the

bound GAG concentration to 105 ± 6 μg GAG/mg agarose ($n = 3$ membranes). Shortening the duration of the three aqueous washes to a total of 15 min increased the bound GAG concentration to 110 ± 1 μg GAG/mg agarose ($n = 2$). However, no further increase was measured for the combined effects of 0 °C and 15 min wash time in Procedure II (102 ± 2 μg GAG/mg agarose, $n = 2$). A number of activation process parameters had little or no effect on the bound GAG concentration of the membranes over the ranges studied: CDAP concentration (0.05–0.2 g/gel), agarose type (I-B or IV), agarose concentration (2–4 v/v %), mixing duration following TEA addition (2–5 min), duration of protonation wash (10–30 min), and exposure to air (0–10 min). Increasing the acid concentration from 0.05 N to 0.2 N during protonation significantly decreased the bound GAG concentration (by 33%).

The temperature and duration of the aqueous wash preceding coupling affected the final bound GAG concentration by changing the concentration of active sites available at the start of coupling. Temperature and duration were studied further by assaying the active sites on the activated membranes. First, the effect of process duration was considered by measuring the active-site content of gels during protonation, aqueous wash and GAG coupling at 4 °C. One batch of membranes contained 2300 nmol cyanate esters/mg agarose shortly after activation, but only 2100 nmol/mg after 20 min of aqueous washing and 1500 nmol/mg at the beginning of coupling (values are averages of duplicate samples). The degradation of active sites continued in the coupling solution, with 100 nmol/mg remaining after 45 h in 4 °C blank coupling solution (0.1 M $NaHCO_3$).

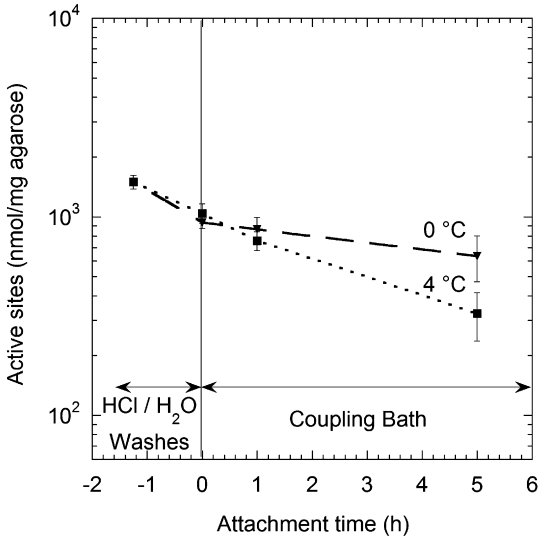

Figure 2. Concentration of active cyanate ester as a function of time, at 0 °C and 4 °C. Symbols are the mean of duplicate samples; error bars are the range. All samples were activated in the same batch and treated identically until coupling.

To understand the 50% increase in the bound GAG concentration at 0 °C versus 4 °C, the kinetics of active-site degradation at these two temperatures was studied. A batch of gels was activated, then split into two groups which were placed in 4 °C or 0 °C blank coupling solutions. As seen in Figure 2, the active sites degraded three times faster in the 4 °C solutions than in the 0 °C solutions. The first-order rate constants for the decay were 0.24 ± 0.02 h^{-1} at 4 °C and 0.08 ± 0.03 h^{-1} at 0 °C. Temperature variations over a much broader range than this have been found to have little effect on agarose structure,[22] indicating that the increase in bound GAG content at 0 °C was mainly due to the reduced rate of active-site degradation.

3.2. Effect of coupling conditions on yield

We were unable to find any variation of conditions in the coupling reaction that would provide a significant increase (>25%) in the bound GAG concentration of the membranes, when chondroitin sulfate (CS) was used. When a 15 kDa heparin was used in place of the 50 kDa CS, the bound GAG concentration on a molar basis was nearly four times higher, although the concentration on a mass basis was similar (78 ± 12 μg heparin/mg agarose, $n = 3$, versus 68 ± 8 μg CS/ mg agarose). A number of process conditions had little or no effect (<25%) on the bound CS concentration over the ranges investigated: pH of the coupling solution (7.0–9.0), tempera-

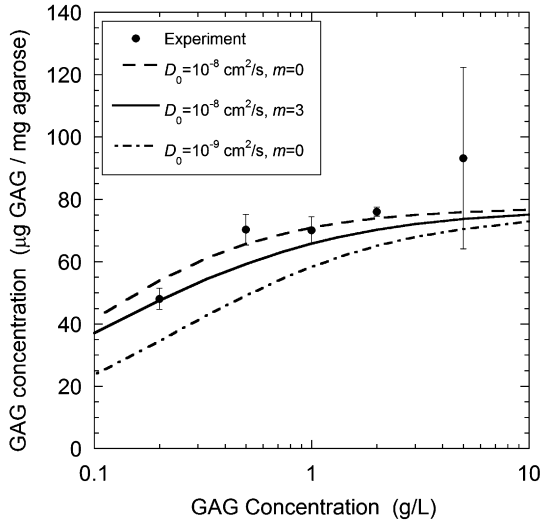

Figure 3. Bound GAG concentration of gels as a function of the GAG (chondroitin sulfate) concentration in the attachment solution. In this and subsequent plots, the mass of bound GAG is expressed relative to that of dry agarose. The symbols are data points, and the curves are model predictions based on various assumptions concerning the GAG diffusivity in the gels. Symbols represent the mean of duplicate samples; error bars indicate the range. The solid curve corresponds to a diffusivity that depends on the concentration of bound GAG. In this and subsequent plots where the coupling time is not specified, the mass of bound GAG in the simulations is that at steady state.

ture of the coupling solution (0–22 °C), and orbital mixing speed (0–200 rpm). Two variations resulted in a significant decrease in the GAG coupling yield: use of salts other than $NaHCO_3$ (60–65% decrease for both bicine and sodium phosphate) and higher salt concentrations (70–75% decrease for 0.5–2.0 M). As illustrated in Figure 3, experiments performed with GAG concentrations of 0.2–5 g/L in the attachment solution showed a marked decrease in the bound GAG concentration at concentrations lower than our standard value of 1 g/L, but no significant increase at higher concentrations. The time-dependent behavior of GAG coupling is shown in Figure 4, which indicates that the coupling

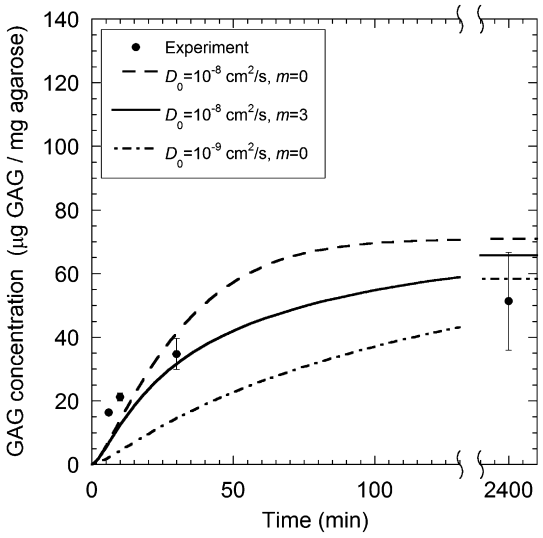

Figure 4. Measured and predicted GAG concentration of gels as a function of coupling time. The symbols are data points and the curves are model predictions based on various assumptions concerning the GAG diffusivity in the gels. Symbols represent the mean of duplicate samples; error bars indicate the range.

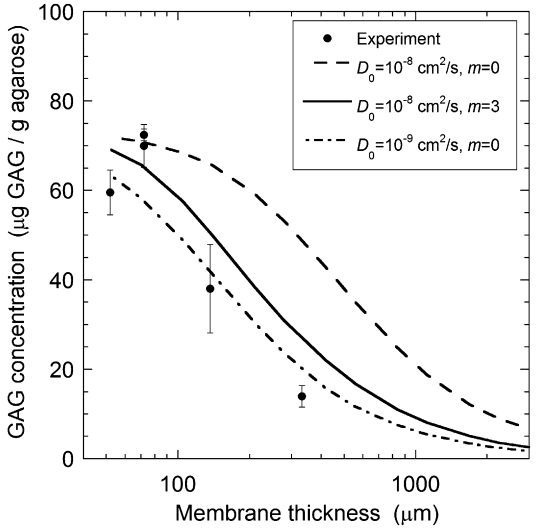

Figure 5. Measured and predicted GAG concentration of gels as a function of membrane thickness. The symbols are data points and the curves are model predictions based on various assumptions concerning the GAG diffusivity in the gels. The error bars represent one standard deviation, for $n = 3$.

capacity of the membranes activated by Procedure I was reached in about 30 min; a much longer coupling time had little benefit. As shown in Figure 5, the concentration of bound GAG decreased for gels thicker than 70 μm, whereas there was no increase for thinner gels.

3.3. Bound GAG distribution

The concentration of bound GAG decreased from 68 ± 8 μg GAG/mg agarose for 70-μm thick membranes to 14 ± 2 μg GAG/mg agarose for 310–360-μm thick membranes ($n = 3$), which suggested that the bound GAG was not uniform throughout the membrane thick-

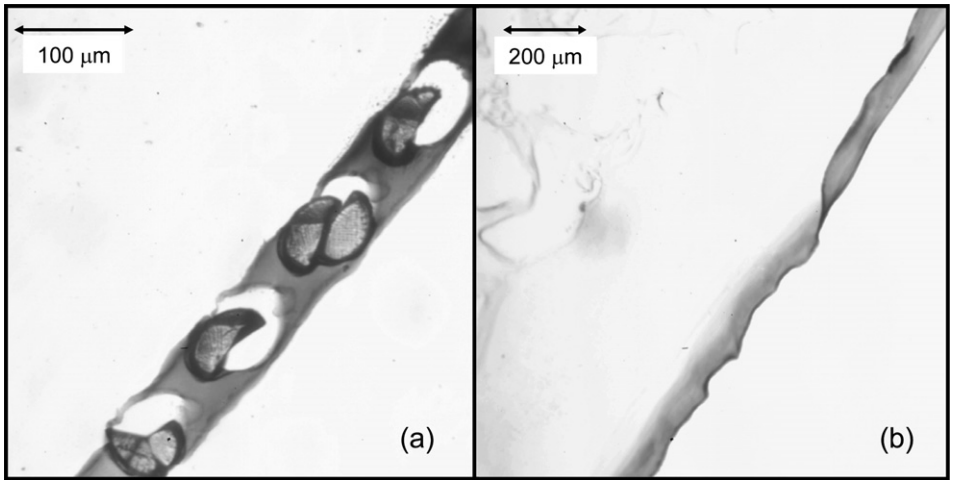

Figure 6. Cross-sections of agarose–GAG membranes after toluidine staining of GAG. (a) A standard, supported membrane of 70-μm thickness (as determined both prior to and after cryosectioning). The holes and oblong objects are due to the polyester support mesh. The bound GAG concentration, as determined from other gels from the same batch, was 77 ± 4 μg GAG/mg agarose ($n = 2$). (b) A gel of about 3-mm thickness, without a supporting mesh. The bound GAG along the edge of the gel is stained purple, while the toluidine dye was washed away from the core of the gel (upper left). The penetration depth of the bound GAG is approximately 50–70 μm.

ness. Stained cryosections were used to address this issue more directly. As shown in Figure 6a, toluidine staining of GAG in a 70-μm membrane (synthesized with Procedure I) resulted in a uniform color throughout the gel. As shown in Figure 6b, in a 3-mm gel (synthesized under the more favorable activating conditions of Procedure II), there was staining only along the edges. The absence of color in the interior of the thick gel confirms that the dye did not bind significantly to agarose, allowing it to be washed away where GAG was absent. Based on Figure 6b and other similar images, the penetration depth of bound GAG was estimated as 50–70 μm. Penetration over that distance from each membrane surface is consistent with the uniform color in Figure 6a.

4. Discussion

4.1. Significant activation and coupling parameters

The objectives of increasing the concentration of bound GAG while maintaining homogeneity were achieved for gel thicknesses $\leqslant$70 μm by increasing the concentration of active sites. That was done by adjusting the duration and temperature of aqueous exposure prior to coupling. Varying numerous other process parameters resulted either in insignificant changes or decreases in the binding yield. It was unsurprising that the agarose concentration had little effect on the bound GAG content, given the small variations in diffusivities of macromolecules within the limited range of agarose concentrations examined.[23]

The process was kinetically rather than stoichiometrically limited, in that the reagents were in 10–10,000-fold excess relative to the bound GAG content. The results are consistent with the reaction conditions mentioned by others to have improved or worsened ligand attachment to cyano-activated carbohydrates, such as changes in HCl concentration,[4] duration of activation reaction,[4,24] coupling pH,[25] ligand concentration,[7] and coupling duration.[7] While binding yield was reported previously to be linearly dependent on CDAP concentration when CDAP was stoichiometrically limiting, the insensitivity of the bound GAG content to the CDAP concentration in the current procedure is likely due to the molar excess of CDAP relative to agarose hydroxyl groups.[4] The effects of certain other parameters that were investigated, such as the thickness of the gel substrate, the ionic strength during coupling, and the temperature during coupling, had not been reported previously.

4.2. Active-site degradation

The cyanate ester degradation rate of 0.24 h^{-1} at 4 °C reduced the active-site content by 20% during the 45 min wash preceding coupling (80% site preservation). It was anticipated that this degradation would be reduced by shortening the wash to 15 min (94% preservation), lowering the temperature to 0 °C (94%), or reducing both the time and temperature (98%), and that slowing the degradation of active sites would improve the yield of bound GAG. This was confirmed, in that the shortened time and lower temperature increased the bound GAG concentration by 62% and 54%, respectively, although no further increase was measured for the combined effects. These rates of active site loss should be applicable to agarose activated by any cyanylating agent, not just CDAP, since all generate active cyanate esters which may degrade into an inert carbamate.

In that there was a 1000-fold excess of active sites relative to the moles of bound GAG, one might expect the binding of GAG to be independent of process changes affecting active-site concentration. Thus, the concomitant increases of active sites and bound GAG at lower process temperatures were surprising. Our explanation for this apparent contradiction is that only a small fraction of active sites were sterically accessible to the GAG, and that increasing the total number of active sites caused a proportionate increase in the number of accessible ones. Agarose forms a complex gel structure in which numerous polysaccharide chains associate side-by-side to form fibrils, and the fibrils intertwine in junction zones during gelation.[26–29] While 10% of the hydroxyl groups on agarose were activated, it is likely that a large fraction of those active sites were inaccessible to large GAG molecules, contributing to the 0.1% binding yield for the 50 kDa chondroitin sulfate. More active sites should be accessible to smaller molecules, in agreement with the higher molar yield that we found for heparin (15 kDa; 0.4% binding yield) and the still higher yield reported previously for aminocaproic acid (131 Da; 24% binding yield).[4]

4.3. Bound GAG distribution

The average GAG concentration decreased from 68 μg GAG/mg agarose for 70-μm thick membranes to 14 μg/mg for 310–360-μm thick membranes. However, the bound GAG concentrations of 50-μm and 70-μm thick gels were statistically indistinguishable. The visual penetration depth of bound GAG of approximately 50–70 μm, on the same order as an average membrane thickness, confirms that GAG was hindered from binding to the core of the membranes for the thicker gels. Therefore, a homogeneous bound GAG concentration was achievable, but only for gels no thicker than our standard ones.

4.4. Modeling

The initial concentration of active cyanate esters, the GAG concentration in solution, the duration of the cou-

pling reaction, and the membrane thickness were all found to influence the bound GAG concentration. Stained cross-sections showed that GAG did not bind to the core of thick membranes. A mathematical model of ligand diffusion and binding (Section 2.8) was developed to explain these trends. The model describes the concentrations of free GAG, active sites, and bound GAG as functions of position and time during the coupling step. Given the local concentrations at any instant, the overall content of bound GAG could be computed as a function of time.

Most parameters in the model could be estimated independently, with baseline values as given in Table 1. The concentration of GAG in bulk solution (C_{GS}) and the gel thickness (δ) were known for each experiment. Following methods similar to those used previously for other macromolecules,[30] data for GAG in unactivated 3 vol % agarose gels (not shown) indicated that the agarose–water partition coefficient (K) was close to unity. The initial concentration of active sites (C_{A0}) and the rate of active-site degradation at 4 °C (k_2) were known from results described above. The fraction of active sites sterically available for binding (ϕ) was estimated from C_{A0} and the amount of GAG bound to thin gels at long exposure times. The rate constant for GAG binding (k_1) was calculated from the amount bound at short times, when the concentration of active sites was near its initial value and the bound GAG concentration was low. Interestingly, our apparent rate constant for binding (ϕk_1) is similar to that reported for the immobilization of heparinase on agarose.[20]

The diffusivity of GAG within the gels was the most uncertain parameter. Some guidance for estimating the value in the absence of bound GAG (D_0) is provided by data for other macromolecules of roughly similar molecular weight in agarose, including dextrans, Ficolls, and proteins.[23,31,32] However, the hydrodynamic radii of GAGs in solution are almost twice those of spherical Ficolls or proteins of similar molecular weight, suggesting that the GAG diffusivity in agarose may be considerably lower. Accordingly, a range of D_0 values was tested (Table 1). An additional parameter, m, was used to model the effect of bound GAG on the diffusivity of free GAG (Eq. 8). For $m = 0$ the diffusivity was constant, whereas for $m > 0$ it declined with increases in the concentration of bound GAG, and therefore varied with position and time.

Table 1. Baseline parameter values used in simulations of GAG binding

Parameter	Value
C_{GS}	2×10^{-8} mol/mL (=1 g/L)
C_{A0}	4×10^{-5} mol/mL
δ	7×10^{-3} cm
D_0	10^{-9}–10^{-7} cm^2/s
m	0–3
K	1
ϕ	1.2×10^{-3}
k_1	4×10^{4} mL mol^{-1} s^{-1}
k_2	5×10^{-5} s^{-1}

In general, the data were found to be inconsistent with any single, constant value of the GAG diffusivity. The simulations agreed best with the bound GAG concentrations at short times and for low solution GAG concentrations when the diffusivity was assumed to be 10^{-7}–10^{-8} cm^2/s (Figs. 3 and 4), whereas the results for thicker membranes suggested a diffusivity as low as 10^{-9} cm^2/s (Figs. 5 and 7). However, all of the results could be reconciled by assuming that the diffusivity of free GAG decreased as the concentration of bound GAG increased, such that $m = 3$. It is reasonable to suppose that bound GAG would create both steric[33] and electrostatic[34] hindrances to diffusion of free GAG, and that these hindrances would become increasingly severe as the coupling step proceeds. Thus, the apparent diffusivities should be largest for short times and low solution GAG concentrations, as observed.

As seen in Figure 3, the model with a concentration-dependent diffusivity predicted the observed decrease in the bound GAG concentration for GAG solution concentrations below 1 g/L. Because the bound GAG concentration was calculated to be relatively insensitive to solution concentration above 1 g/L, the model confirmed that further increases in the concentration of the attachment solution are not a viable method of increasing the concentration of bound GAG. The results in Figure 4 concerning the time course of binding were also well explained. That is, most of the GAG attachment was predicted to occur within 30 min, as observed.

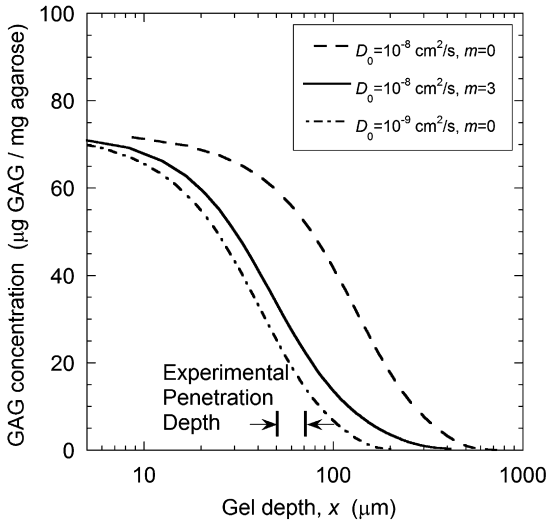

Figure 7. Predicted concentration of bound GAG as a function of depth for agarose–GAG gels of indefinitely large thickness. The depth is the distance from the surface of the gel, and the thickness used in the calculations was such that the concentration of bound GAG at the membrane center was at least two orders of magnitude smaller than that at the surface.

The model with a concentration-dependent diffusivity also accounted well for the effects of membrane thickness, as shown in Figure 5. A comparison of the curves for $D_0 = 10^{-8}$ cm^2/s and $m = 0$ or $m = 3$ suggests that diffusivity reductions due to bound GAG played an important role in lessening the binding in thicker gels. The effects of gel thickness are illustrated also by predictions of bound GAG concentration as a function of position in a gel of indefinitely large thickness, as shown in Figure 7. As expected, the lower the diffusivity, the smaller the penetration depth. Assuming that the visual penetration depth is approximately the position at which the bound GAG concentration is one quarter of the surface concentration, the penetration depth for the semi-infinite gel with concentration-dependent diffusivity is 83 μm, consistent with the experimental penetration depth of 50–70 μm. The model also predicts that the bound GAG concentration in a 70-μm thick gel would decrease by only 18% between the gel surface and gel center, which would not be noticeable in a stained cryosection such as that in Figure 6a.

4.5. Kinetic considerations in selecting binding conditions

An analysis of time scales for the coupling step provides general insight into conditions that will yield high and/or spatially uniform concentrations of bound ligand. The three time scales of interest are those for diffusion of free ligand (t_D), binding of ligand to active sites (t_1), and decay of active sites (t_2), which are given by

$$t_D = \frac{\delta^2}{4D_0}, \quad t_1 = \frac{1}{k_1 K C_{GS}}, \quad t_2 = \frac{1}{k_2}. \tag{3}$$

The diffusional time scale is based on half of the membrane thickness, which is the maximum distance that the free ligand must traverse. From the parameters in Table 1 with $D_0 = 10^{-8}$ cm^2/s, the values of these time scales for our conditions were $t_D = 20$ min, $t_1 = 21$ min, and $t_2 = 330$ min.

Increasing the concentration of bound ligand requires increases in the yield per active site and/or the number of active sites. To fully utilize the available sites (i.e., maximize the yield), the binding reaction must be fast relative to active-site degradation, or $t_1 \ll t_2$. Because t_1 was already an order of magnitude smaller than t_2 under our baseline conditions (21 min compared with 330 min), there was little opportunity to improve the yield per active site. That is, increasing C_{GS} above the baseline value of 1 g/L would decrease t_1, and lowering the coupling temperature would increase t_2 (by decreasing k_2), but little gain in yield could be expected because the reaction time scales were already different enough. However, as shown in Figure 3, the yield could be worsened by a sufficient lowering of C_{GS} (e.g., $t_1 = 105$ min at 0.2 g/L). In that $t_1 \ll t_2$ was already satisfied by the baseline conditions, thereby maximizing the yield, the only option for increasing the concentration of bound GAG was to increase the initial concentration of active sites (ϕC_{A0}). That is what was done by lowering the temperature and shortening the wash periods prior to coupling.

Of course, the duration of the coupling period had to be sufficient to fully utilize the active sites. With the lifetime of the active sites controlled mainly by GAG binding (rather than by active-site degradation), this required that the coupling time significantly exceed t_1. As t_1 for our baseline conditions was only 21 min, one expects little advantage in extending the coupling reaction over the full 16 h that is often suggested in published procedures. This is in agreement with the results in Figure 4.

The bound ligand concentration will be nearly uniform if diffusion occurs more rapidly than binding, or $t_D \ll t_1$. That is, if free ligand penetrates the entire matrix before an appreciable amount reacts, it will equilibrate with the external solution, and a spatially uniform concentration of bound ligand will result. However, our finding that GAG binding in 70-μm membranes was homogeneous even for t_D comparable to t_1 (both about 20 min) indicates that this inequality is overly conservative; while sufficient, it is not necessary. The reason this criterion is conservative is that, whereas ligand bound near the gel surface may impede the diffusion of free ligand (as apparently happened in our system), even as binding near the surface saturates it may not fully prevent free ligand from penetrating well into the interior (as also seems to have been true for our system). Thus, the importance of having a small value of t_D is affected by the extent that bound ligand 'clogs' the gel, an effect captured by the full model which predicted the homogeneity of thin membranes and the penetration depth into very thick membranes.

A similar analysis of time scales can be applied to systems with different geometries, ligands, or kinetics. For spherical beads, the bead radius can be substituted for the membrane half-thickness. As already mentioned, the rate constant reported here for the degradation of cyanate esters should be applicable to other cyanylating agents. This and previous work[20] provide estimates also for the fraction of accessible active sites and the rate constant for ligand binding; if desired, those estimates can be refined using short- and long-time binding data from the system of interest, as done here. Thus, if estimates of the ligand diffusivity are available, favorable synthesis conditions can be identified for a wide range of coupled ligand–agarose applications.

References

1. Larsen, K.; Thygesen, M. B.; Guillaumie, F.; Willats, W. G. T.; Jensen, K. J. *Carbohydr. Res.* **2006**, *341*, 1209–1234.

2. Cuatrecasas, P. *J. Biol. Chem.* **1970**, *245*, 3059–3065.
3. Porath, J. *Methods Enzymol.* **1974**, *34*, 13–30.
4. Kohn, J.; Wilchek, M. *Appl. Biochem. Biotechnol.* **1984**, *9*, 285–305.
5. Miller-Andersson, M.; Borg, H.; Andersson, L. *Thromb. Res.* **1974**, *5*, 439–452.
6. Nadkarni, V. D.; Pervin, A.; Lindardt, R. J. *Anal. Biochem.* **1994**, *222*, 59–67.
7. Lees, A.; Nelson, B. L.; Mond, J. J. *Vaccine* **1996**, *14*, 190–198.
8. Afanassiev, V.; Hanemann, V.; Wölfl, S. *Nucleic Acids Res.* **2000**, *28*, e66.
9. Axén, R.; Porath, J.; Ernback, S. *Nature* **1967**, *214*, 1302–1304.
10. Iverius, P. H. *Biochem. J.* **1971**, *124*, 677–683.
11. Kato, I.; Anfinsen, C. B. *J. Biol. Chem.* **1969**, *244*, 5849–5855.
12. Porath, J.; Axén, R.; Ernback, S. *Nature* **1967**, *215*, 1491–1492.
13. de Bernardo, S.; Weigele, M.; Toome, V.; Manhart, K.; Leimgruber, W.; Böhlen, P.; Stein, S.; Udenfriend, S. *Arch. Biochem. Biophys.* **1974**, *163*, 390–399.
14. Toome, V.; de Bernardo, S.; Manhart, K.; Weigele, M. *Anal. Lett.* **1974**, *7*, 437–443.
15. Toome, V.; Manhart, K. *Anal. Lett.* **1975**, *8*, 441–448.
16. Johnson, E. M.; Berk, D. A.; Jain, R. K.; Deen, W. M. *Biophys. J.* **1995**, *68*, 1561–1568.
17. Johnston, S. T.; Deen, W. M. *J. Membr. Sci.* **1999**, *153*, 217–279.
18. Smith, P. K.; Mallia, A. K.; Hermanson, G. T. *Anal. Biochem.* **1980**, *109*, 466–473.
19. Kohn, J.; Wilchek, M. *Anal. Biochem.* **1981**, *115*, 375–382.
20. Bernstein, H.; Yang, V. C.; Langer, R. *Biotechnol. Bioeng.* **1987**, *30*, 196–207.
21. Masaro, L.; Zhu, X. X. *Prog. Polym. Sci.* **1999**, *24*, 731–775.
22. Mackie, W.; Sellen, D. B.; Sutcliffe, J. *Polymer* **1978**, *19*, 9–15.
23. Johnson, E. M.; Berk, D. A.; Jain, R. K.; Deen, W. M. *Biophys. J.* **1996**, *70*, 1017–1026.
24. March, S. C.; Parikh, I.; Cuatrecasas, P. *Anal. Biochem.* **1974**, *60*, 149–152.
25. Shafer, D. E.; Toll, B.; Schuman, R. F.; Nelson, B. L.; Mond, J. J.; Lees, A. *Vaccine* **2000**, *18*, 1273–1281.
26. Attwood, T. K.; Nelmes, B. J.; Sellen, D. B. *Biopolymers* **1988**, *27*, 201–212.
27. Djabourov, M.; Clark, A. H.; Rowlands, D. W.; Ross-Murphy, S. B. *Macromolecules* **1989**, *22*, 180–188.
28. Ratajska-Gadomska, B.; Gadomski, W. *J. Chem. Phys.* **2004**, *121*, 12583–12588.
29. Waki, S.; Harvey, J. D. *Biopolymers* **1982**, *21*, 1909–1926.
30. Kosto, K. B.; Panuganti, S.; Deen, W. M. *J. Colloid Interface Sci.* **2004**, *277*, 404–409.
31. Bertini, S.; Bisio, A.; Torri, G.; Bensi, D.; Terbojevich, M. *Biomacromolecules* **2005**, *6*, 168–173.
32. Lebrun, L.; Junter, G. A. *Enzyme Microb. Technol.* **1993**, *15*, 1057–1062.
33. Kosto, K. B.; Deen, W. M. *AIChE J.* **2004**, *50*, 2648–2658.
34. Hirota, N.; Kumaki, Y.; Narita, T.; Gong, J. P.; Osada, Y. *J. Phys. Chem. B* **2000**, *104*, 9898–9903.